RESEARCH PAPER

The transient receptor potential channel antagonist SKF96365 is a potent blocker of low-voltage-activated T-type calcium channels

A Singh[1], ME Hildebrand[2], E Garcia[1] and TP Snutch[1]

[1]*Michael Smith Laboratories, University of British Columbia, Vancouver, British Columbia, Canada, and* [2]*Neuromed Pharmaceuticals, Vancouver, British Columbia, Canada*

Background and purpose: SKF96365 (SKF), originally identified as a blocker of receptor-mediated calcium entry, is widely used diagnostically, as a blocker of transient receptor potential canonical type (TRPC) channels. While SKF has been used as a tool to define the functional roles of TRPC channels in various cell and tissue types, there are notable overlapping physiological and pathophysiological associations between TRPC channels and low-voltage-activated (LVA) T-type calcium channels. The activity of SKF against T-type Ca channels has not been previously explored, and here we systematically investigated the effects of SKF on recombinant and native voltage-gated Ca channel-mediated currents.
Experimental approach: Effects of SKF on recombinant Ca channels were studied under whole-cell patch clamp conditions after expression in HEK293 cells. The effect of SKF on cerebellar Purkinje cells (PCs) expressing native T-type Ca channels was also assessed.
Key results: SKF blocked recombinant Ca channels, representative of each of the three main molecular genetic classes (Ca_V1, Ca_V2 and Ca_V3) at concentrations typically utilized to assay TRPC function (10 µM). Particularly, human $Ca_V3.1$ T-type Ca channels were more potently inhibited by SKF (IC_{50} ~560 nM) in our experiments than previously reported for similarly expressed TRPC channels. SKF also inhibited native $Ca_V3.1$ T-type currents in a rat cerebellar PC slice preparation.
Conclusions and implications: SKF was a potent blocker of LVA T-type Ca channels. We suggest caution in the interpretation of results using SKF alone as a diagnostic agent for TRPC activity in native tissues.
British Journal of Pharmacology (2010) **160,** 1464–1475; doi:10.1111/j.1476-5381.2010.00786.x

Introduction

SKF96365 (SKF) was originally described as a selective blocker of receptor-mediated Ca entry (RMCE) over Ca release from internal stores in non-excitable cells such as platelets, endothelial cells and neutrophils (Merritt *et al.*, 1990). In the interim, SKF has been used extensively to elucidate the contributions of RMCE or store-operated Ca entry (SOCE) in many physiological processes. Transient receptor potential canonical type (TRPC) channels (channel nomenclature follows Alexander *et al.*, 2009) have been demonstrated to

mediate RMCE and in some cases SOCE (alternatively known as capacitative Ca entry) (Clapham *et al.*, 2001; Moran *et al.*, 2004), and are thought to be a major molecular target underlying inhibition by SKF (Kiselyov *et al.*, 1998; Zhu *et al.*, 1998; Rychkov and Barritt, 2007). Although less bulky than classical voltage-gated Ca channel antagonists (Merritt *et al.*, 1990; Doering and Zamponi, 2003) (Figure 1), SKF has been shown to inhibit high-voltage-activated (HVA) L-type Ca channels in GH3 pituitary cells and smooth muscle cells (Merritt *et al.*, 1990). Additional reports indicate further blocking effects of SKF on K channels (Schwarz *et al.*, 1994; Liu *et al.*, 2007), the sarcoplasmic reticulum Ca-ATPase (Mason *et al.*, 1993), nicotinic receptors (Hong and Chang, 1994) and voltage-gated Na channels (Hong *et al.*, 1994).

Accumulating lines of evidence indicate that in many cell and tissue types, TRPC channel family members share

SKF96365 block of T-type calcium channels
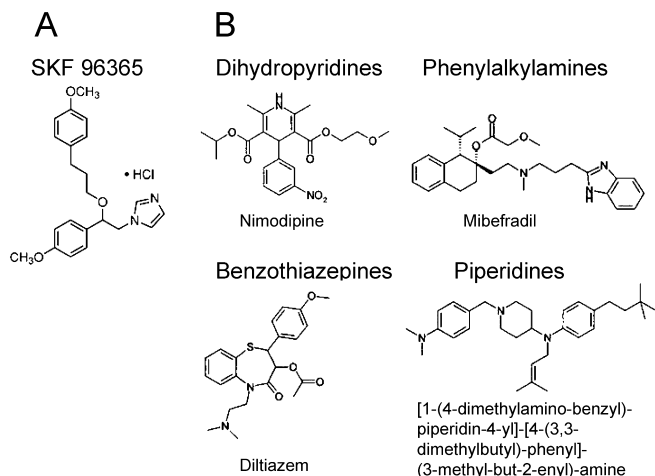A Singh *et al*
1465

Figure 1 Structure of SKF96365 compared to voltage-activated calcium channel antagonists. (A) SKF96365 (1{β-[3-(4-methoxyphenyl)propoxyl]-4-methoxyphenethyl}-1*H*-imidazole hydrochloride) consists of an alkylated imidazole ring which can be present in the phenylalkylamine class of Ca channel antagonists such as mibefradil. (B) Structure of various classes of Ca channel antagonists. Dihydropyridines typically consist of a core pyridine structure, phenylalkylamines consist of at least one phenyl ring linked to an amine head group by an alkyl chain, benzothiazepines have a rigid bulky tricyclic core with several substituents. Diphenylbutylpiperidines typically have one or more heterocyclic amine piperidine.

functional roles with low-voltage-activated (LVA) T-type Ca channels and also that both are over/re-expressed in certain pathological conditions such as cancer (Panner *et al.*, 2005; Bomben and Sontheimer, 2008) and hypertension (Self *et al.*, 1994; Liu *et al.*, 2009). In many instances, the functional contribution of the TRPC channels has in part been assessed pharmacologically by blockade with SKF. SKF in the micromolar range (2–100 μM) inhibits Ca influx through TRPC channels heterologously expressed in human embryonic kidney cells (HEK293), as well as in many native systems (Okada *et al.*, 1998; Zhu *et al.*, 1998; Wang and Poo, 2005; Bomben and Sontheimer, 2008; Romero-Mendez *et al.*, 2008). Given that both TRPC and voltage-gated Ca channels mediate Ca influx across overlapping membrane potentials, together with previous reports of SKF blockade of HVA L-type Ca channels, the use of SKF as a diagnostic tool for native TRPC channel activity requires further investigation. This becomes even more important in the case of T-type Ca channels which can generate Ca influx at resting membrane potentials and may contribute to processes attributed to TRPC such as the maintenance of intracellular Ca levels (Kim *et al.*, 2007).

To the best of our knowledge, there has been no systematic study reporting the effects of SKF on the major classes of HVA and LVA Ca channels. In the present report, we have studied the effects of SKF on recombinant T-type, P/Q-type, N-type and L-type Ca channels. We have also utilized brain slices to investigate the effect of SKF on native $Ca_V3.1$ T-type Ca currents in rat cerebellar Purkinje cells (PCs). The results show that SKF is a potent blocker of LVA and HVA Ca channels. A detailed analysis of recombinant LVA $hCa_V3.1$ T-type Ca channels shows that high-affinity blockade ($IC_{50} = 563$ nM) occurs largely in a state-independent manner. SKF also inhibits native $Ca_V3.1$ T-type currents in cerebellar PCs. Overall, our

study found that SKF blocked T-type Ca channels more potently than recombinant TRPC channels similarly expressed in heterologous systems (Boulay *et al.*, 1997; Okada *et al.*, 1998; Zhu *et al.*, 1998), and at similar or lower concentrations in native systems (Kim *et al.*, 2003; Wang and Poo, 2005; Bomben and Sontheimer, 2008; Romero-Mendez *et al.*, 2008). Given the sometimes overlapping physiological contributions of TRPC and T-type Ca channels, we conclude that caution should be exercised when utilizing SKF as the sole pharmacological agent to assess the contributions of RMCE and SOCE in native systems.

Methods

Cell culture and transient expression
HEK293 were grown in standard Dulbecco's modified Eagle's medium (DMEM) supplemented with 10% fetal bovine serum and 50 units·mL^{-1} penicillin/streptomycin. The cells were grown up to ~80% confluence and maintained at 37°C in a humidified incubator with 95% room air and 5% CO_2. Stable cell lines (in HEK293/tsa-201) expressing human $Ca_V3.1$, $Ca_V3.2$, $Ca_V3.3$ T-type (denoted as $hCa_V3.X$), rat brain $Ca_V3.1$, $Ca_V2.1$ P/Q-type (+ $β_4$ + $α_2δ_2$) and $Ca_V2.2$ N-type (+ $β_{1b}$ + $α_2δ_2$) channels (denoted as $rCa_VX.X$) were kindly provided by Neuromed Pharmaceuticals. Stable cell lines were maintained in supplemented DMEM containing appropriate antibiotics for selection: zeocin (25 μg·mL^{-1}) for $hCa_V3.1$; hygromycin (150 μg·mL^{-1}), blasticidine (10 μg·mL^{-1}), geniticin (600 μg·mL^{-1}) for $hCa_V3.2$; hygromycin (300 μg·mL^{-1}) for $hCa_V3.3$; zeocin (50 μg·mL^{-1}) for $rCa_V3.1$; hygromycin (150 μg·mL^{-1}), blasticidine (10 μg·mL^{-1}), zeocin (200 μg·mL^{-1}) for $rCa_V2.1$ P/Q-type channel; and hygromycin (300 μg·mL^{-1}), blasticidine (10 μg·mL^{-1}), zeocin (300 μg·mL^{-1}) for $rCa_V2.2$ N-type channel. Stable cell lines were plated on glass coverslips 24 h before recordings. $hCa_V3.2$, $rCa_V2.1$ and $rCa_V2.2$ channels were induced with doxycycline at the time of plating. Rat brain $Ca_V1.2$ L-type Ca channels (denoted as $rCa_V1.2$) were expressed transiently in HEK293 cells together with $α_2δ$ and $β_{2A}$ subunits using the standard Ca phosphate method. Cells transfected with $rCa_V1.2$ channel complex were plated onto glass coverslips after 24 h of transfection and recorded 24 h after plating. As a reporter for transient L-type Ca channel expression, the CD8 marker plasmid was co-transfected.

Electrophysiological recordings from HEK293 cells and data analysis
Macroscopic currents were recorded using the whole-cell patch clamp technique with the external recording solution containing (in mM): 2 $CaCl_2$, 1 $MgCl_2$, 10 HEPES, 40 tetraethylammonium chloride (TEA Cl), 92 CsCl, 10 glucose, pH 7.4 with CsOH, ~305 mOsm, and the internal pipette solution containing (in mM): 130 Cs-methanesulphonate, 11 EGTA, 10 HEPES, 2 $MgCl_2$, 4 Mg-ATP, 0.3 Na-GTP, pH 7.2 with CsOH, ~290 mOsm. Macroscopic currents were recorded using Axopatch 200B amplifiers (Axon Instruments, Foster City, CA, USA), controlled and monitored with Pentium IV personal computers running pClamp software version 9 (Axon Instru-

1466
SKF96365 block of T-type calcium channels
A Singh *et al*

ments). Fire-polished patch pipettes (borosilicate glass) had typical resistances of 3–5 MΩ when containing internal solution. The bath was connected to the ground via an Ag–AgCl pellet. Data were low-pass filtered at 2 kHz using the built-in Bessel filter of the amplifier and sampled at 10–20 kHz. The amplifier was also used for capacitive transient and series resistance compensation between 70 and 85% on each cell. Leak subtraction of leakage currents was either performed on-line using a P/4 protocol or else performed with Clampfit (Axon Instruments) during off-line analysis. All recordings were performed at room temperature (20–22°C). Current–voltage (I–V) relationships were obtained by holding the cells at a potential of −100 mV (for T-type and N-type channels) or −80 mV (for L-type and P/Q-type channels) before applying 150 ms pulses to potentials from −80 to +10 mV every 5 s in 5 mV increments. The potential that elicited peak current (V_{max}) was obtained from this protocol and used as the test pulse voltage (peak potential) in subsequent protocols. Series resistance was also monitored with a 5 ms hyperpolarizing pulse immediately before the test pulse to ensure that this variable was relatively constant, and any changes in peak current levels were not because of significant changes in series resistance. Effects of different concentrations of SKF were investigated using 120 ms steps to peak potential every 5 s (0.2 Hz) from a holding potential of −100 mV (for T-type and N-type) or −80 mV (for L-type and P/Q-type). To quantify the per cent of channel inhibition during SKF or control solution perfusion, the following equation was used: % inhibition = [1 − ($I_{(t)}/I_{max}$)] × 100, where I_{max} is the peak current magnitude at equilibrium (averaged 2–5 values) and $I_{(t)}$ is the equilibrium current after block.

I–V relationships were fitted with the modified Boltzmann equation, $I = [G_{max} \times (V_m − E_{rev})]/\{1 + \exp[(V_m − V_{0.5a})/K_a]\}$, where V_m is the test potential, $V_{0.5a}$ is the half-activation potential, E_{rev} is the extrapolated reversal potential, G_{max} is the maximum slope conductance and K_a reflects the slope of the activation curve. Microcal Origin (version 7.5, Northampton, MA, USA) was used to analyse data and generate figures. Dose–response curves were fitted by non-linear curve fitting of the Hill equation to the data using the Origin software. Steady-state inactivation of hCa$_V$3.1 channels was measured by holding the cells for 200 ms at various indicated potentials followed by a 90 ms test pulse to V_{max}. Steady-state inactivation curves were analysed using the following Boltzman equation: $I = I_{ss} + (1 − I_{ss})/[1 + \exp(V − V_{0.5,inact}/k_{inact})]$, where I is the peak current amplitude, I_{ss} is the non-inactivating fraction, V is the membrane potential, $V_{0.5,inact}$ is the half-inactivation potential and k_{inact} is the slope factor. Tail currents were measured over a range of negative potentials from −150 to −60 mV in 10 mV increments after a 9 ms depolarizing pulse to −30 mV.

Electrophysiological recordings from cerebellar slices
All animal care and experimental procedures were done in accordance with the recommendations of the Canadian Council on Animal Care and the animal care regulations and policies of the University of British Columbia. Cerebellar slices were obtained from male Wistar rats (9–11 days old) as previously described (Hildebrand *et al.*, 2009). Briefly, the animals were anaesthetized with halothane, and decapitated, with the head being immediately chilled in a protective sucrose cutting solution containing (in mM): 50 sucrose, 92 NaCl, 5 KCl, 26 NaHCO$_3$, 1.25 NaH$_2$PO$_4$, 0.5 CaCl$_2$, 7 MgSO$_4$, 15 glucose, 1 kynurenate and bubbled with 95% O$_2$/5% CO$_2$. All dissection and slicing were performed in this solution. The cerebellar vermis was then removed with a scalpel and glued in the sagittal orientation to the stage of a Vibratome 1500 Sectioning System (St Louis, MO, USA). Sagittal slices (300 μm) were cut from the cerebellar vermis and transferred to a recovery chamber with bicarbonate-buffered saline (BBS) solution at 34°C, containing (in mM): 125 NaCl, 3 KCl, 26 NaHCO$_3$, 1.25 NaH$_2$PO$_4$, 2 CaCl$_2$, 1 MgCl$_2$, 20 glucose, 1 kynurenate and 0.1 picrotoxin, and bubbled with 95% O$_2$/5% CO$_2$. Once slicing was complete, the heating in the water bath containing the recovery chamber was turned off, and the recovery chamber was allowed to cool down to room temperature.

For electrophysiological recordings, the cerebellar slices were transferred to a Warner recording chamber (Warner Instruments, Hamden, CT, USA) and perfused with bubbled BBS external solution containing 300 nM tetrodotoxin, 5 mM TEA Cl, 1 mM 4-aminopyridine and 30 μM CdCl$_2$ to enable recordings of isolated T-type Ca channel currents. Cerebellar PCs were visually identified using a Zeiss Axioskop 2 with IR-DIC optics (Carl Zeiss, Inc., Gottinger, Germany), and whole-cell patch clamp recordings from PCs were performed using a Multiclamp 700B amplifier (Molecular Devices, Sunnyvale, CA, USA). The internal pipette solution contained (in mM): 140 Cs-methanesulphonate, 5 TEA Cl, 0.5 MgCl$_2$, 10 HEPES, 4 MgATP, 0.5 Na$_3$GTP and 0.3 EGTA, pH adjusted to 7.3, ~290 mOsm. Borosilicate glass pipettes had typical resistances of 4–6 MΩ when filled with internal solution. To ensure the quality of the space clamp, modulatory effects were studied on T-type currents of moderate amplitude elicited every 10 s from a holding potential of −75 mV (with a 500 ms pre-pulse to −90 mV to remove inactivation) to depolarizing 200 ms test pulses ranging between −46 and −35 mV. Cells with leak current (voltage-clamped baseline current recorded from the holding potential period) above 300 pA at V_h = −75 mV were discarded. Data were low-pass filtered at 2 kHz using the built-in Bessel filter of the amplifier, with sampling at 20 kHz. Series resistance was compensated between 70 and 75% on every cell, while liquid junction potentials that were calculated to be approximately 9 mV (at 22°C) were left uncorrected. Leak subtraction was performed off-line using Clampfit 9 (Molecular Devices).

Data analysis
All averaged data are presented as mean ± SEM. Means were tested for significance with Student's two-tailed *t*-test, with $P < 0.05$ considered significant. P values were reported only where significance was observed.

Materials
A 100 mM stock of SKF96365 (Tocris Bioscience, Ellisville, MO, USA) was prepared in autoclaved water, aliquoted, stored at −20°C and used within 2 months. Dilutions in recording

SKF96365 block of T-type calcium channels
A Singh *et al*
1467

solution were made from the stock on the day of experiments to reach the final concentration. Gravity-driven perfusion occurred at a rate of ~2 mL·min⁻¹ in a coverslip chamber of 300 µL liquid volume.

Results

SKF potently and reversibly inhibits recombinant T-type calcium channels

LVA T-type Ca channels and TRPC channels co-exist in many cell types where they play significant roles in relation to many physiological and pathophysiological conditions. Pharmacological blockade has been extensively used to explore the functional implications of Ca influx through both T-type and TRPC channels as it relates to various Ca-mediated signalling and excitatory pathways. Pharmacological blockade with SKF has been used to identify TRPC channels in many cell types, and we wished to determine whether T-type Ca channels could be affected by SKF. We initially utilized HEK293 cells stably expressing hCa$_V$3.1 channels which under whole-cell patch clamp conditions generated currents ranging from ~800 to 1000 pA (Figure 2A; in 2 mM extracellular Ca). Perfusion of 1 µM SKF reversibly inhibited 86.3 ± 0.1% (*n* = 15) of the current, reaching maximum inhibition in 6–7 min. Application of 2.5 µM (data not shown) and 10 µM SKF both completely abolished hCa$_V$3.1 currents within 3–4 min (*n* = 6–7). Figure 2A shows representative inward Ca current (I_{Ca}) traces of block by 1 and 10 µM SKF, and subsequent recovery from inhibition upon washing with control external solution. Figure 2D shows the mean time-course of inhibition by 1 and 10 µM SKF on the same cells (*n* = 6), while Figure 2G shows a representative time-course of block and recovery from inhibition. Examining the other two T-type isoforms, hCa$_V$3.2 (99.9% inhibition, Figure 2B,E,H and Figure 3D, *n* = 8) and hCa$_V$3.3 (97.2% inhibition, Figure 2C,F,I and Figure 3D, *n* = 7) channels also showed potent block by 10 µM SKF that reached steady-state inhibition in approximately 5 min. As evident from the current traces, the macroscopic activation and inactivation kinetics of all three T-type Ca channels were not altered during SKF blockade (Figure 2A–C). For hCa$_V$3.1 currents, tau activation and inactivation values were compared before and after perfusion of 1 µM SKF (Figure 2A, control, τ-act = 1.9 ± 0.1 ms, *n* = 15; 1 µM SKF, τ-act = 1.6 ± 0.8 ms, *n* = 15; control τ-inact = 11.9 ± 0.4 ms, *n* = 15; 1 µM SKF τ-inact = 12.3 ± 0.5 ms, *n* = 15). For hCa$_V$3.2, tau activation and inactivation values were compared at 50% inhibition during perfusion of 10 µM SKF (Figure 2B, control, τ-act = 3.0 ± 0.1 ms, *n* = 8; 10 µM SKF, τ-act = 2.7 ± 0.1 ms, *n* = 8; control τ-inact = 15.8 ± 0.9 ms, *n* = 8; 10 µM SKF τ-inact = 17.3 ± 1.0 ms, *n* = 8). Macroscopic current kinetics also remain unchanged for hCa$_V$3.3 currents compared at 50% inhibition during perfusion of 10 µM SKF (Figure 2C, control, τ-act = 11.5 ± 0.6 ms, *n* = 7; 10 µM SKF, τ-act = 11.7 ± 0.8 ms, *n* = 7; control τ-inact = 140.6 ± 2.8 ms, *n* = 7; 10 µM SKF τ-inact = 137.0 ± 9.9 ms, *n* = 7).

SKF inhibits recombinant P/Q-, N- and L-type calcium channels

Potent inhibition of LVA T-type Ca channels by SKF motivated us to test whether SKF also blocks recombinant neuronal HVA

Ca channels. Examining HEK293 cells stably expressing rCa$_V$2.1 and rCa$_V$2.2 channels showed that 10 µM SKF nearly completely abolished both P/Q-type and N-type currents within approximately 4 min (Figure 3A,B, *n* = 6, 5 respectively). Blockade was only partially reversible as inhibition by 10 µM SKF did not exhibit 100% wash-out, and which may be due to partially irreversible drug binding and/or channel run-down over the longer time period required for wash-out of SKF (Figure 3A,B, right panels). Some run-down during perfusion was also observed for rCa$_V$2.2 channels during control perfusion (Figure 3B, left panel, see 0–0.5 min). The macroscopic activation kinetics of rCa$_V$2.1 currents were not altered during SKF blockade (compared at 50% inhibition; control, τ-act = 3.8 ± 0.7 ms, *n* = 6; 10 µM SKF, τ-act = 3.9 ± 0.4 ms, *n* = 6). Although the τ-inact was not calculated because of less apparent inactivation, the rCa$_V$2.1 inactivation kinetics did not seem to differ during SKF perfusion (Figure 3A, right panel). The macroscopic activation and inactivation kinetics of rCa$_V$2.2 currents were also not altered during SKF blockade (compared at 50% inhibition; control, τ-act = 1.6 ± 1.2 ms, *n* = 5; 10 µM SKF, τ-act = 1.4 ± 0.2 ms, *n* = 5; control, τ-inact = 81.4 ± 6.9 ms, *n* = 5; 10 µM SKF, τ-inact = 66.9 ± 6.5 ms, *n* = 5).

We also examined the effects of 10 µM SKF on a member of the third evolutionary branch of mammalian Ca channel family, the rCa$_V$1.2 L-type. L-type Ca channel blockade by 50 µM SKF in smooth muscle cells was reported in the original SKF study by Merritt *et al.* (1990). In contrast to the relatively fast time-course of SKF block of P/Q-type channels, 10 µM SKF inhibited rCa$_V$1.2 L-type channels slowly (*t*1/2 to maximum block: 1.5 ± 0.2 min (*n* = 6) for rCa$_V$2.1 P/Q-type versus 3.3 ± 0.5 min (*n* = 6) for rCa$_V$1.2 L-type, *P* < 0.01), reaching ~90% inhibition in about 6 min (Figure 3C, left panel, grey curve, *n* = 6). Under our experimental conditions, we observed a slow constant run-down of rCa$_V$1.2 currents over the same time period (Figure 3C, left panel, black curve, *n* = 7). Therefore, in order to estimate the mean % block of rCa$_V$1.2 by 10 µM SKF (Figure 3D), we subtracted the mean % run-down during 6 min of control perfusion from the mean % block observed during 10 µM SKF perfusion (Figure 3D). Although we did not observe any reversibility of SKF block on rCa$_V$1.2 Ca channels for up to 4 min of control perfusion, it is possible that the recovery is too slow and in part masked by slow channel run-down, and therefore is not observed in our experimental conditions. Alternatively, SKF may bind irreversibly to HVA Ca channels such as rCa$_V$1.2, rCa$_V$2.1 and rCa$_V$2.2 (Figure 3, right panels). As for other HVA Ca channels, the activation kinetics of rCa$_V$1.2 channels were not altered during SKF block (compared at 50% inhibition; control, τ-act = 1.1 ± 0.1 ms, *n* = 10; 10 µM SKF, τ-act = 1.3 ± 0.1 ms, *n* = 6), and the inactivation kinetics do not appear to be altered by SKF block (Figure 3B, right panel). Comparison of the mean percentage block by 10 µM SKF across the different major classes of voltage-gated Ca channels indicated extensive block by SKF of the three isoforms of T-type Ca channels (97–100%), the rCa$_V$2.1 P/Q-type Ca channel (97%) and the rCa$_V$2.2 N-type channel (99.2%). Blockade was slightly less for the rCa$_V$1.2.L-type Ca channel (70%) (Figure 3D). As T-type Ca channels and TRPC channels share a subset of expression profiles and physiological roles, we further investigated the mechanism of block

Figure 3 SKF blocks rCa$_V$2.1 P/Q-type, rCa$_V$2.2 N-type and rCa$_V$1.2 L-type calcium channels. Mean time-course of current inhibition of recombinant rCa$_V$2.1 P/Q-type (A) and rCa$_V$2.2 N-type Ca channels (B) by 10 μM SKF. Currents were elicited by depolarization to V_{max} (0–5 mV for P/Q and 20 mV for N-type, 120 ms duration) applied every 5 s from a holding potential of −80 mV for P/Q-type and −100 mV for N-type. Right panel shows representative I_{Ca} during 120 ms depolarizations before, after perfusion of 10 μM SKF and after wash-out with control solution, as indicated. The rates of channel activation and inactivation did not differ before, during or after perfusion of SKF (see text for statistics). (C) Mean time-course of current inhibition of recombinant rCa$_V$1.2 L-type Ca channels by 10 μM SKF (grey curve). Black curve represents the mean time-course of run-down during control perfusion. Right panel shows representative I_{Ca} during 120 ms depolarizations before and after perfusion of 10 μM SKF (see text for statistics). (D) Comparison of the effect of 10 μM SKF on four classes of Ca channels. Data for T-type Ca channels were taken from Figure 2. For calculating the mean % block of rCa$_V$1.2 current by 10 μM SKF, the mean % run-down during 6 min of control perfusion (black plot in B) was subtracted from the mean % block observed during 10 μM SKF perfusion (grey plot in B). Error bars indicate SEM, Ns are given in parentheses.
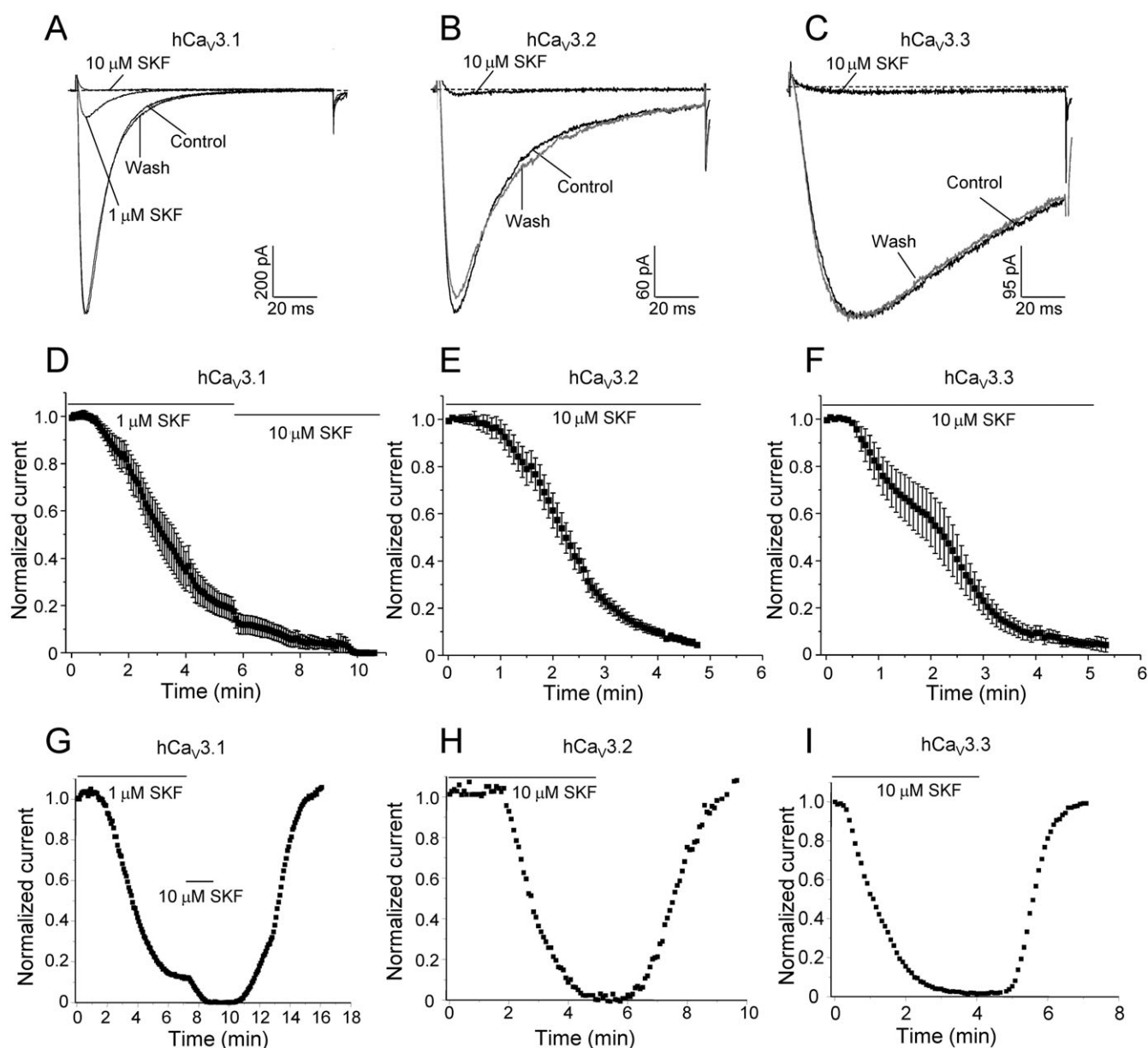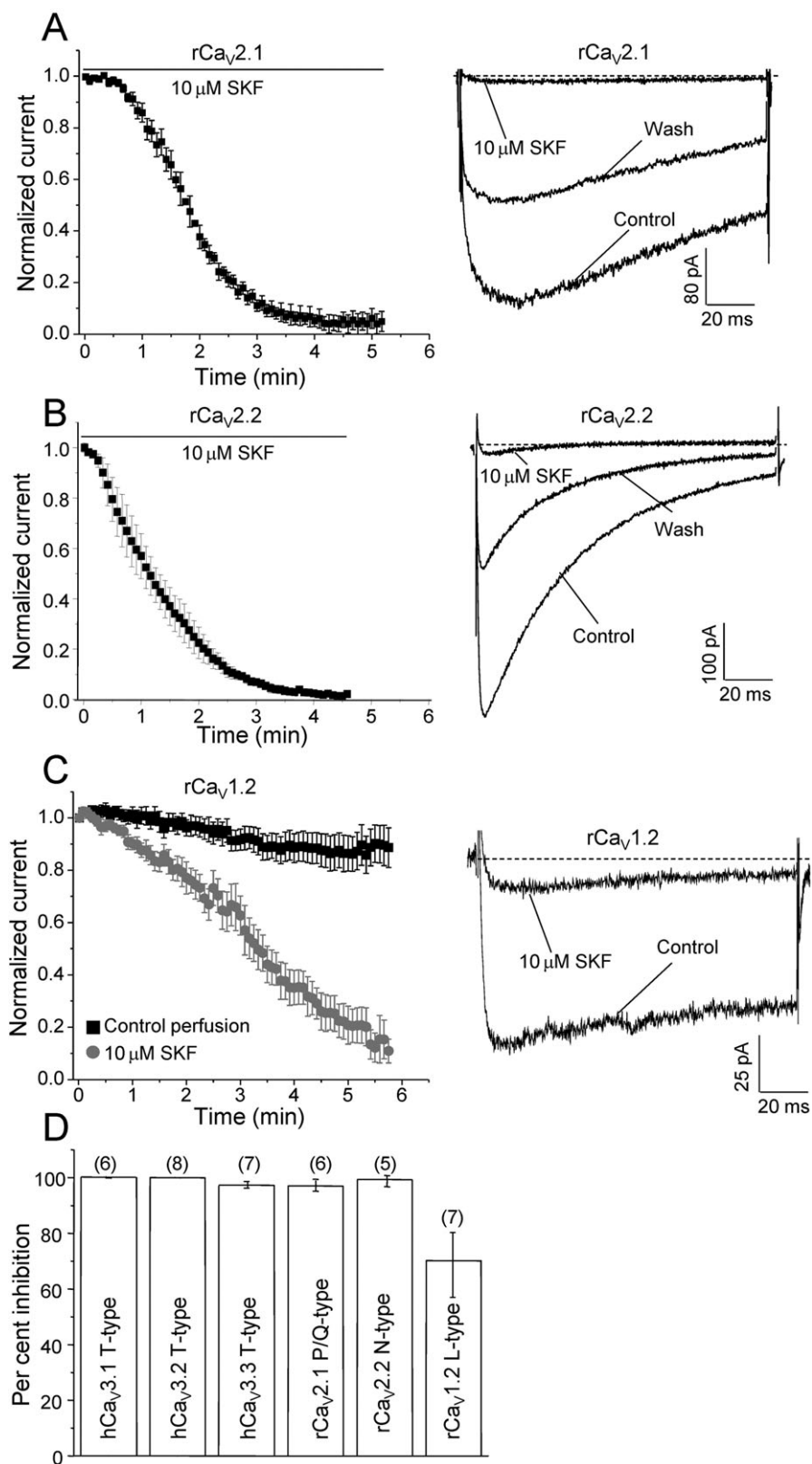

Figure 2 SKF is a potent blocker of T-type calcium channels. Representative I_{Ca} during 120 ms depolarizations to V_{max} from a holding potential of −100 mV before (control), after perfusion with different concentrations of SKF (as indicated) and after wash-out with control solution (wash) for hCa$_V$3.1 (A), hCa$_V$3.2 (B) and hCa$_V$3.3 (C). Traces shown here after complete wash-out of SKF are taken at 6.5, 5.5 and 3.3 min for A, B and C respectively. (D) Mean time-course of I_{Ca} inhibition by 1 and 10 μM SKF for hCa$_V$3.1. Mean time-course of I_{Ca} inhibition by 10 μM SKF for hCa$_V$3.2 (E) and hCa$_V$3.3 (F). Representative time-course of current inhibition and recovery from inhibition for hCa$_V$3.1 (G), hCa$_V$3.2 (H) and hCa$_V$3.3 (I). Currents were elicited by depolarization to V_{max} (−35 to −25 mV, 120 ms duration) applied every 5 s from a holding potential of −100 mV. The apparent rates of channel activation and inactivation did not differ before, during or after perfusion of SKF (see text for statistics).
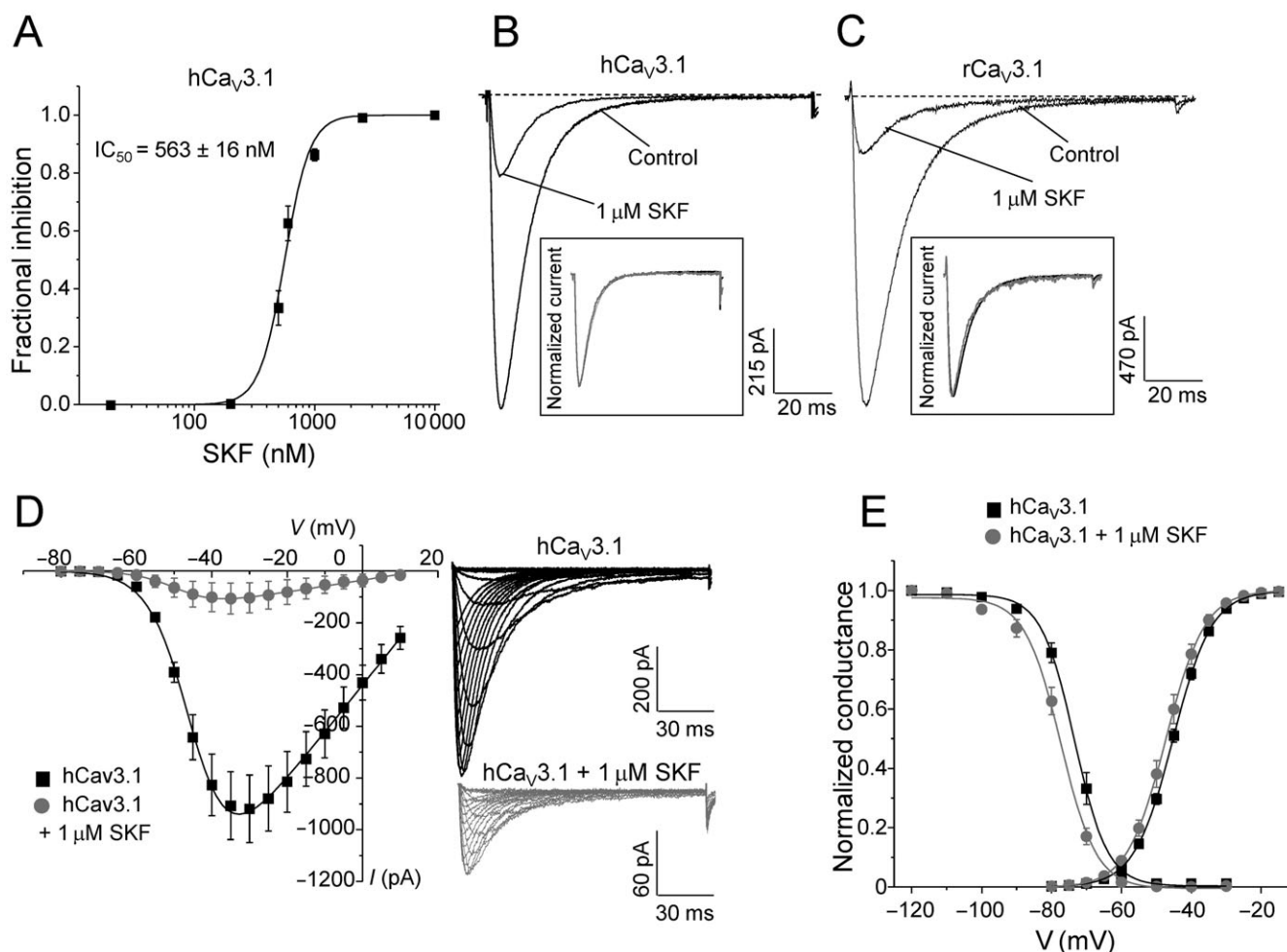
Figure 4 Mechanism of block of SKF on hCa$_V$3.1 calcium channels. (A) Dose–response curve of SKF on recombinant hCa$_V$3.1 channels (n = 5–15). (B) Representative I_{Ca} during 120 ms depolarizations to V_{max} (−30 mV) from a holding potential of −100 mV before and after perfusion of 1 μM SKF as indicated. Inset shows normalized traces for comparison of kinetics (see text for statistics). (C) Representative I_{Ca} during 120 ms depolarizations to V_{max} (−30 mV) from a holding potential of −100 mV before and after perfusion of 1 μM SKF for rCa$_V$3.1 as indicated. Inset shows normalized traces for comparison of kinetics (see text for statistics). (D) Mean I–V before and after 1 μM SKF block (control n = 8, 1 μM SKF n = 6). SKF inhibited hCa$_V$3.1 currents at all test potentials. Right panel shows representative I_{Ca} traces (150 ms steps to potentials ranging from −80 to +10 mV in 5 mV increments) before (black) and after perfusion with 1 μM SKF (grey). (E) Normalized mean peak conductance at various test potentials before and after perfusion of 1 μM SKF. $V_{0.5act}$ in control conditions was not significantly different from after SKF block (see text for $V_{0.5act}$ statistics). Steady-state inactivation curves before and after 1 μM SKF block. Solid lines are fits to the Boltzmann relationship (see Methods). $V_{0.5inact}$ after 1 μM SKF was 4 mV more negative than control (see text for $V_{0.5inact}$ statistics).

of SKF on the hCa$_V$3.1 subtype of T-type channel. In order to rule out possible species-dependent differences in SKF sensitivity across various classes of voltage-gated Ca channels, we also compared SKF effects on hCa$_V$3.1 versus rCa$_V$3.1 (see next section).

SKF inhibits hCa$_V$3.1 T-type calcium channels dose-dependently and independent of the channel state
Examining the dose–response relationship of SKF block of hCa$_V$3.1 channels showed a half maximal effect (IC$_{50}$) at 563 ± 16 nM (n = 5–15, Figure 4A). The dose–response curve was quite steep (Hill coefficient 4.2 ± 0.7, n = 5–15), and block by SKF at lower concentrations was slow, taking up to 10–12 min to reach the maximal effect. Figure 4B inset shows representative normalized traces before and after 1 μM SKF block, confirming that SKF did not significantly alter hCa$_V$3.1 acti-

vation or inactivation kinetics as previously described. The IC$_{50}$ of SKF block on rCa$_V$3.1 was very similar to hCa$_V$3.1 (rCa$_V$3.1, IC$_{50}$: 579 ± 77 nM, n = 3–5, data not shown). As for hCa$_V$3.1 channels, macroscopic activation and inactivation kinetics of rCa$_V$3.1 channels were not altered during 1 μM SKF perfusion (Figure 4C, control, τ-act = 2.2 ± 0.2 ms, n = 6; 1 μM SKF, τ-act = 1.9 ± 0.1 ms, n = 6; control τ-inact = 15.6 ± 0.7 ms, n = 6; 1 μM SKF τ-inact = 15.0 ± 1.0 ms, n = 6). Finding no observable difference across species for Ca$_V$3.1 T-type Ca channels, we investigated the mechanism of SKF block on hCa$_V$3.1 T-type Ca channels.

The hCa$_V$3.1-mediated Ca currents were inhibited at all potentials, indicative of a voltage-independent blocking mechanism (Figure 4D). The half-maximal voltage of activation ($V_{0.5act}$) was unaffected by perfusion of 1 μM SKF (Figure 4D; control, $V_{0.5act}$ = −45.2 ± 0.5 mV, n = 13; 1 μM SKF, $V_{0.5act}$ = −47.3 ± 0.9 mV, n = 6). Unlike that for inhibitors that

stabilize the inactivated state of Ca channels such as endogenous lipoamino acids (Barbara *et al*., 2009) and endocannabinoids (Chemin *et al*., 2001), SKF only slightly shifted the steady-state of inactivation to more negative potentials (Figure 4E; control, $V_{0.5inact} = -73.3 \pm 1.0$ mV, $n = 9$; 1 µM SKF, $V_{0.5inact} = -77.5 \pm 1.0$ mV, $n = 6$; $P = 0.02$). This small shift in the steady-state inactivation also slightly shifted the window current to more negative potentials. Although statistically significant, this small shift in the steady-state inactivation alone does not likely explain the marked inhibition of hCa$_V$3.1 channels by SKF.

A hallmark of T-type Ca channels is their slow deactivation kinetics, which results in large tail currents that can underlie after depolarizing potentials and bursting behaviour. To examine the effects of SKF on the voltage dependence of deactivation kinetics, we measured tail currents over a range of membrane potentials from –150 to –60 mV after a 9 ms depolarizing pulse to –30 mV (Orestes *et al*., 2009). We did not observe any significant difference in the macroscopic deactivation kinetics of hCa$_V$3.1 currents (Figure 5A,B).

SKF tonically inhibits hCa$_V$3.1 T-type calcium channels
The largely voltage-independent mechanism of blockade prompted us to test whether SKF blocks hCa$_V$3.1 channels in the closed/resting state. We examined the relative contributions of tonic and use-dependent block of hCa$_V$3.1 currents by SKF. In one set of experiments, we used a protocol consisting of recording a train of depolarizations pulsed at a frequency of 0.2 Hz in the presence of 1 µM SKF until steady-state inhibition was reached (~6 min in our conditions, Figure 5C,E) in order to assess the total inhibition by 1 µM SKF. In a separate set of experiments, 1 min of SKF application was followed by a rest period, during which time the holding potential was set to –100 mV (Figure 5D,F). At –100 mV, most hCa$_V$3.1 channels would be in the closed state. After a 4 min resting period, an identical train of voltage clamp depolarizations was applied at a frequency of 0.2 Hz. Total blockade was considered to be the proportional difference between the first trace and the last trace after steady-state inhibition. The same amount of current inhibition (compared after 6 min of 1 µM SKF exposure) was observed under both conditions (0.2 Hz depolarizations, % inhibition = 81.2 ± 0.1%, $n = 8$; holding at –100 mV, % inhibition = 81.6 ± 0.04%, $n = 6$, Figure 5), suggesting that SKF inhibits T-type Ca channels in a tonic (state-independent) manner. Thus, it appears that SKF cannot be classified as an open channel blocker, and there is no strong evidence that it selectively stabilizes the inactivated state of hCa$_V$3.1 channels. In this regard, the mechanism of action of SKF appears different from other LVA Ca channel blockers such as mibefradil (Jimenez *et al*., 2000) and isoflurane (Orestes *et al*., 2009). The tonic blockade indicates that SKF interacts with T-type Ca channels independent of their functional state, and thus T-type channels would be likely to be inhibited under most experimental conditions used to functionally measure TRPC channels and also independent of the applied stimulus.

SKF inhibits native Ca$_V$3.1 T-type calcium currents in cerebellar PCs
Although heterologous systems such as HEK293 cells offer the advantage of studying specific drug actions in a defined environment, the observed effects may not reflect all the characteristics of the native system. In order to validate and complement the data from recombinant T-type Ca channels expressed in HEK293 cells, we studied the effects of SKF on rat cerebellar PCs that we have previously shown endogenously express Ca$_V$3.1 T-type channels (Hildebrand *et al*., 2009). To ensure that native T-type currents were well clamped and not contaminated by HVA Ca currents, we used depolarizing steps (average step = –43 ± 2 mV, $n = 5$) that elicited submaximal T-type Ca currents (Figure 6A; average T-type current amplitude = 238.2 ± 20.4 pA, $n = 5$). SKF inhibition was determined by applying the depolarizing pulses every 10 s. Figure 6A,B shows representative current traces and a representative time-course of inhibition of native Ca$_V$3.1 T-type currents by 30 µM SKF and subsequent wash-out respectively. Perfusion of 30 µM SKF reversibly inhibited 60.1 ± 1.8% ($n = 5$, $P < 0.01$) of the native T-type current reaching maximum inhibition in approximately 8 min of SKF application (Figure 6C). As observed for recombinant hCa$_V$3.1 channels, SKF did not significantly alter macroscopic native T-type current activation or inactivation kinetics (control, τ-act = 4.0 ± 0.3 ms, $n = 5$; 30 µM SKF, τ-act = 3.7 ± 0.2 ms, $n = 5$; control τ-inact = 29.5 ± 1.6 ms, $n = 5$; 30 µM SKF τ-inact = 30.4 ± 2.9 ms, $n = 5$). In addition, perfusion of 50 µM SKF blocked over 90% of the native T-type current in PCs (data not shown). The higher SKF doses required for the inhibition of PC native T-type currents compared to exogenous Ca$_V$3.1 currents in HEK293 cells is a common phenomenon when comparing recombinant pharmacology data with *in vitro* slice data wherein both drug access and non-specific binding can alter access to the target. In addition, as native neuronal Ca currents likely represent a combination of functionally distinct splice variants, it is also possible that altered drug sensitivities between assay systems in part reflect differences in target molecules. Nevertheless, the doses used here on PCs are well within the range of SKF concentrations typically used to explore the roles of TRPC/RMCE in many native tissue preparations (Kim *et al*., 2003; Wang and Poo, 2005; Bomben and Sontheimer, 2008; Romero-Mendez *et al*., 2008).

Discussion

Numerous studies investigating the functional roles of TRPC channels and RMCE have utilized SKF blockade as part of their diagnostic criteria. SKF is often used in the concentration range of 2–100 µM with IC$_{50}$ values (where reported) in the range of 5–30 µM (Merritt *et al*., 1990; Okada *et al*., 1998; Zhu *et al*., 1998; Wang and Poo, 2005; Bomben and Sontheimer, 2008; Romero-Mendez *et al*., 2008). Of note, reports show that in a wide variety of cell types including cerebellar PCs, midbrain dopamine neurons, vascular smooth muscle cells, as well as in various pathological states such as hypertrophic heart and gliomas, TRPC channels often co-exist with LVA T-type Ca channels (Kim *et al*., 2003; 2007; Cui *et al*., 2004; Panner *et al*., 2005; Ohba *et al*., 2007; Bomben and
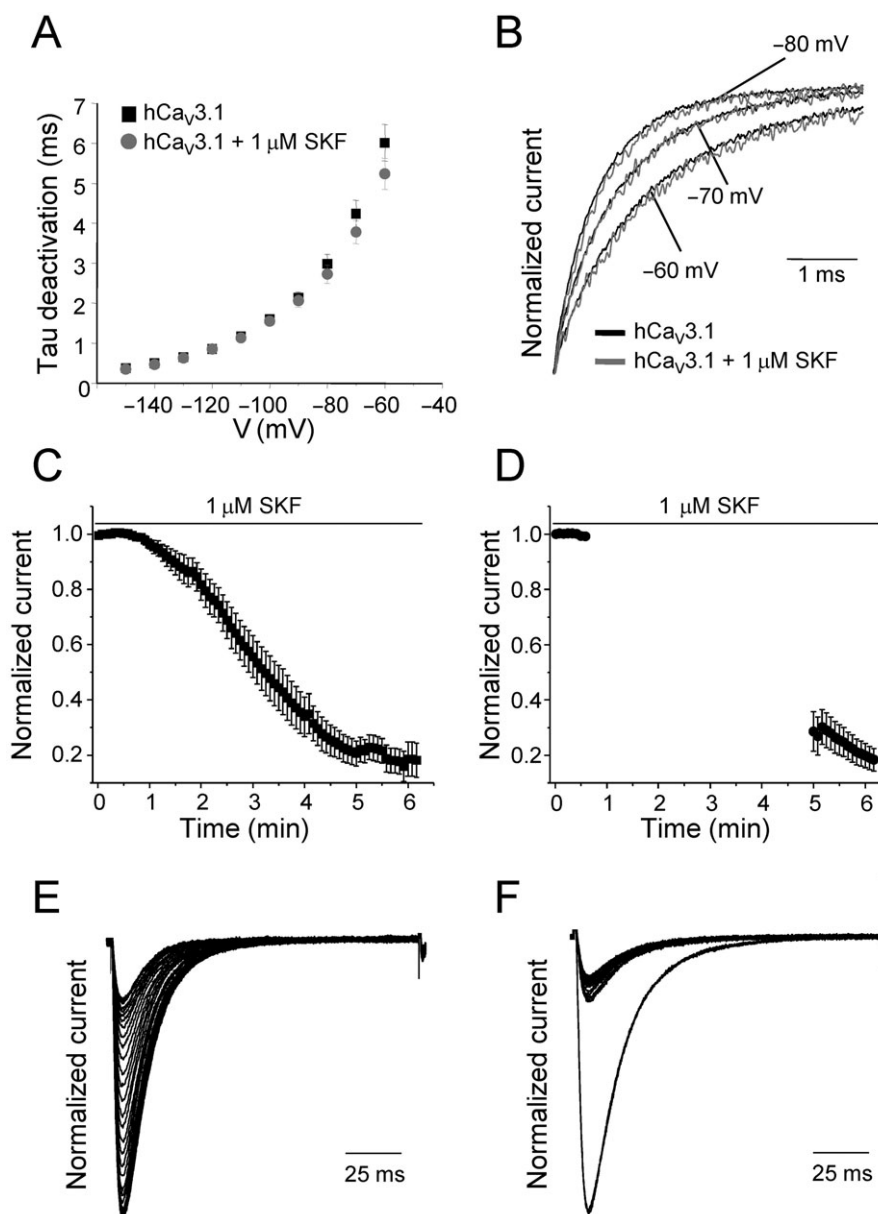
Figure 5 Voltage dependence of deactivation kinetics and tonic block of SKF on hCa$_V$3.1 T-type calcium channels. (A) Mean values of tau deactivation plotted for hCa$_V$3.1 before and after perfusion of 1 μM SKF. The values were obtained by a single exponential fit of the time-course of tail currents at the indicated test voltages. (B) Representative normalized tail current recorded during test voltages of −80, −70 and −60 mV (as indicated) before (black traces) and after perfusion of 1 μM SKF (grey traces). (C) Mean time-course of current inhibition during 0.2 Hz depolarizations to V_{max} in the presence of 1 μM SKF ($n = 8$) to determine the use-dependent block of SKF on hCa$_V$3.1 channels. Currents were elicited as described in Figure 2. The I_{Ca} reached steady-state inhibition in ~6 min. (D) After 1 min of bath application of 1 μM SKF, the channels were held at −100 mV without depolarizations for ~4 min. The depolarizations at 0.2 Hz were resumed after 4 min of rest period to determine tonic blockade of SKF on hCa$_V$3.1 channels ($n = 6$). All data are presented as mean ± SEM. Representative normalized I_{Ca} traces during 6 min of 0.2 Hz depolarizations (E) or when the cells were held at −100 mV (F). Only alternate traces are shown for clarity.

Sontheimer, 2008; Chiang *et al.*, 2009). For example, in one study, inhibition of TRPC channels with 25 μM SKF in malignant gliomas resulted in growth arrest of glioma cells (Bomben and Sontheimer, 2008), while in another study the unequivocal role of T-type Ca channels in glioma and neuroblastoma proliferation using T-type blockers such as mibefradil was shown (Panner *et al.*, 2005). Further, increased Ca entry into vascular smooth muscle from spontaneously hypertensive rats was reduced by 10 μM SKF and attributed to

TRPC3 although up-regulation of T-type Ca channels has also been reported in this system (Self *et al.*, 1994; Liu *et al.*, 2009).

Structurally, SKF contains an alkylated imidazole ring which is also present in the class of compounds called phenylalkylamines known to block both HVA and LVA Ca channels (Figure 1). Interestingly, introduction of a substituted imidazole ring into dihydropyridines has been shown to increase their potency on Ca channels (Davood *et al.*, 2006). While no reports concerning the specific interaction of the
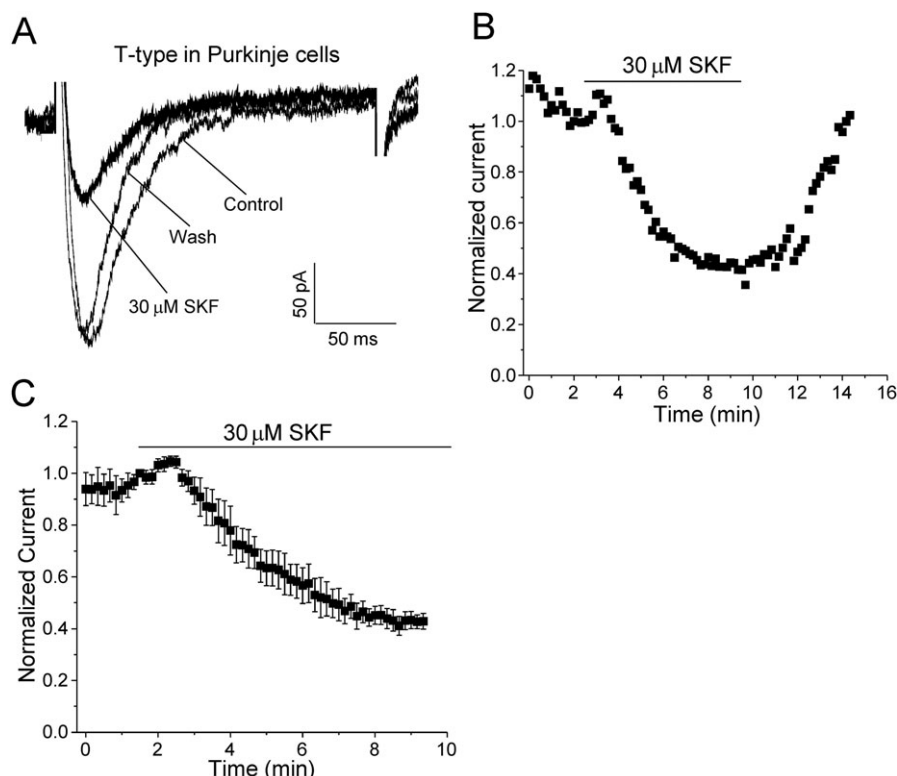
SKF96365 block of T-type calcium channels
A Singh et al
1473

Figure 6 Effect of SKF on native T-type currents in cerebellar PCs. (A) Representative T-type current during 200 ms depolarizations to submaximal test potentials (as described in Methods) before, after perfusion of 30 μM SKF and after wash-out (as indicated). Currents were elicited by 200 ms depolarizations to −45 mV every 10 s from a holding potential of −75 mV (with a 500 ms prepulse to −90 mV to remove inactivation, as described in Methods). The apparent rates of channel activation and inactivation did not vary significantly before or during perfusion of SKF (for statistics, see text). (B) Representative time-course of T-type current inhibition by 30 μM SKF and subsequent wash-out with control solution. (C) Mean time-course of T-type current inhibition by 30 μM SKF (n = 5). The perfusion of 30 μM SKF inhibited 60.1 ± 1.8% of the T-type current during ~8 min of SKF application.

imidazole ring with the structural determinants of Ca channel inhibition have been published, it is possible that SKF inhibits Ca channels in a non-specific, allosteric manner. Although non-specific inhibitory effects of SKF on some HVA Ca channels (Merritt et al., 1990; Chan and Greenberg, 1991; Bannister et al., 2009) and other ion channels (Hong and Chang, 1994; Hong et al., 1994; Schwarz et al., 1994) have been reported, there has been no systematic analysis of the effects of SKF on the voltage-gated Ca channel family and there are no reports concerning T-type Ca channels. Given the co-existence of TRPC channels and other non-selective cation channels together with Ca channels in many native systems, and the non-specific effects of SKF, it is possible that in some studies wherein SKF was used to study RMCE, the roles of voltage-gated Ca channels have been underestimated and/or the contributions of non-selective cation channels might have been overestimated. In the present study, we have systematically determined the effect of SKF on T-, L- N- and P/Q-type Ca channels taking advantage of the HEK293 heterologous expression system, and have focused our studies on T-type Ca channels because of their expression and functional overlap with TRPC channels. We report for the first time that SKF blocks LVA T-type Ca channels even more potently than TRPC channels expressed in HEK293 cells [Figure 4A; IC_{50} ~563 nM vs. IC_{50} ~5 μM for TRPC3 (Zhu et al., 1998)]. At

10 μM, SKF also inhibited HVA P/Q-type (Figure 3A), N-type (Figure 3B) and L-type (Figure 3C) Ca channels by 96.9, 99.2 and 70% respectively.

While HEK293 cells offer many advantages in studying specific drug interactions on exogenously expressed targets, they are likely to differ from native systems because of the expression of specific alternative splice variants, interacting proteins and other factors that might affect channel biophysical properties, pharmacology and modulation. Block of TRPC1 channels by 30–50 μM SKF in cerebellar PCs has revealed their contribution to the slow EPSP generated following mGluR1 receptor activation (Kim et al., 2003). In our examination of PCs, we found that 30 μM SKF blocked approximately 60% of the native T-type current (Figure 6A,C). A recent study from our lab indicated that native $Ca_V3.1$ T-type Ca channels were potentiated by mGluR1 receptor activation in PC spines and underlie fast Ca signalling at parallel fibre–PC synapses (Hildebrand et al., 2009). Thus, in native tissues wherein T-type channels co-exist with TRPC channels, they may both exhibit similar sensitivities to SKF and also might overlap in their contributions towards Ca-dependent signalling pathways. Of note, the concentration of SKF required to block either T-type Ca channels (Figure 6) or TRPC channels (Kim et al., 2003) in cerebellar PCs was much higher compared to doses required to block recombinant Ca channels (Figure 2) or recombinant

TRPC channels (Zhu et al., 1998) expressed in HEK293 cells. It is possible that splice variant differences across species together with other factors such as non-specific drug binding in part explain the different drug potencies when recording native currents. However, our experiments comparing sensitivity of recombinant $hCa_V3.1$ and $rCa_V3.1$ channels expressed in HEK293 cells to SKF (Figure 4B,C) support the view that any species differences alone do not account for the difference in the drug sensitivity.

Based upon our results, it is possible that the full contributions of T-type Ca channels have not been explored in some studies. SKF inhibition of T-type Ca channels was found to be only mildly voltage dependent (Figures 4D,E and 5), suggesting that SKF is likely to block T-type Ca channels under basal conditions such as those used to determine resting Ca influxes and spontaneous Ca oscillations. For example, 10 μM SKF has been used to identify the contribution of non-selective cation channels in maintaining intracellular Ca levels and spontaneous firing in midbrain dopamine neurons (Kim et al., 2007). The window current resulting from T-type Ca channels is well within the range of the resting membrane potential of these neurons. Thus, their contributions to the resting Ca levels should not be ruled out. Indeed, experiments with inorganic ions such as Ni^{2+} and Cd^{2+} (known to block T-type Ca channels) support this notion (Kim et al., 2007). Additionally, the reported inhibition of proliferation of glioma cells by 25 μM SKF may well have resulted from the additive inhibition of both TRPC and T-type Ca channels (Bomben and Sontheimer, 2008). Emerging roles of TRPC and T-type Ca channels in sensing hypoxia also further emphasize the overlapping expression and function of these channels, and that non-specific blockers such as SKF may not be the optimal choice to study TRPC channels in these tissues (Carabelli et al., 2007; Meng et al., 2008).

Taken together, the present study provided evidence that not only did SKF block HVA Ca channels at typically utilized test concentrations, but even more potently inhibited T-type Ca channels than the intended TRPC target. In light of these data, blockade by SKF alone should not be the defining criterion for assessing and interpreting the functional roles of TRPC channels in native systems.

Acknowledgements

Conflicts of interest

The authors do not report any conflicts of interest concerning the contents of the present paper.

References

Alexander SPH, Mathie A, Peters JA (2009). Guide to Receptors and Channels (GRAC), 4th edn. Br J Pharmacol 158: S1–S254.

Bannister RA, Pessah IN, Beam KG (2009). The skeletal L-type Ca(2+) current is a major contributor to excitation-coupled Ca(2+) entry. J Gen Physiol 133: 79–91.

Barbara G, Alloui A, Nargeot J, Lory P, Eschalier A, Bourinet E et al. (2009). T-type calcium channel inhibition underlies the analgesic effects of the endogenous lipoamino acids. J Neurosci 29: 13106–13114.

Bomben VC, Sontheimer HW (2008). Inhibition of transient receptor potential canonical channels impairs cytokinesis in human malignant gliomas. Cell Prolif 41: 98–121.

Boulay G, Zhu X, Peyton M, Jiang M, Hurst R, Stefani E et al. (1997). Cloning and expression of a novel mammalian homolog of Drosophila transient receptor potential (Trp) involved in calcium entry secondary to activation of receptors coupled by the Gq class of G protein. J Biol Chem 272: 29672–29680.

Carabelli V, Marcantoni A, Comunanza V, de Luca A, Diaz J, Borges R et al. (2007). Chronic hypoxia up-regulates alpha1H T-type channels and low-threshold catecholamine secretion in rat chromaffin cells. J Physiol 584: 149–165.

Chan J, Greenberg DA (1991). SK & F 96365, a receptor-mediated calcium entry inhibitor, inhibits calcium responses to endothelin-1 in NG108-15 cells. Biochem Biophys Res Commun 177: 1141–1146.

Chemin J, Monteil A, Perez-Reyes E, Nargeot J, Lory P (2001). Direct inhibition of T-type calcium channels by the endogenous cannabinoid anandamide. EMBO J 20: 7033–7040.

Chiang CS, Huang CH, Chieng H, Chang YT, Chang D, Chen JJ et al. (2009). The Ca(v)3.2 T-type Ca(2+) channel is required for pressure overload-induced cardiac hypertrophy in mice. Circ Res 104: 522–530.

Clapham DE, Runnels LW, Strubing C (2001). The TRP ion channel family. Nat Rev 2: 387–396.

Cui G, Okamoto T, Morikawa H (2004). Spontaneous opening of T-type Ca^{2+} channels contributes to the irregular firing of dopamine neurons in neonatal rats. J Neurosci 24: 11079–11087.

Davood A, Mansouri N, Rerza Dehpour A, Shafaroudi H, Alipour E, Shafiee A (2006). Design, synthesis, and calcium channel antagonist activity of new 1,4-dihydropyridines containing 4-(5)-chloro-2-ethyl-5-(4)-imidazolyl substituent. Arch Pharm 339: 299–304.

Doering CJ, Zamponi GW (2003). Molecular pharmacology of high voltage-activated calcium channels. J Bioenerg Biomembr 35: 491–505.

Hildebrand ME, Isope P, Miyazaki T, Nakaya T, Garcia E, Feltz A et al. (2009). Functional coupling between mGluR1 and Cav3.1 T-type calcium channels contributes to parallel fiber-induced fast calcium signaling within Purkinje cell dendritic spines. J Neurosci 29: 9668–9682.

Hong SJ, Chang CC (1994). Facilitation of nicotinic receptor desensitization at mouse motor endplate by a receptor-operated Ca^{2+} channel blocker, SK & F 96365. Eur J Pharmacol 265: 35–42.

Hong SJ, Lin WW, Chang CC (1994). Inhibition of the sodium channel by SK & F 96365, an inhibitor of the receptor-operated calcium channel, in mouse diaphragm. J Biomed Sci 1: 172–178.

Jimenez C, Bourinet E, Leuranguer V, Richard S, Snutch TP, Nargeot J (2000). Determinants of voltage-dependent inactivation affect mibefradil block of calcium channels. Neuropharmacology 39: 1–10.

Kim SJ, Kim YS, Yuan JP, Petralia RS, Worley PF, Linden DJ (2003). Activation of the TRPC1 cation channel by metabotropic glutamate receptor mGluR1. Nature 426: 285–291.

Kim SH, Choi YM, Jang JY, Chung S, Kang YK, Park MK (2007). Nonselective cation channels are essential for maintaining intracellular Ca^{2+} levels and spontaneous firing activity in the midbrain dopamine neurons. Pflugers Arch 455: 309–321.

Kiselyov K, Xu X, Mozhayeva G, Kuo T, Pessah I, Mignery G *et al*. (1998). Functional interaction between InsP3 receptors and store-operated Htrp3 channels. *Nature* **396**: 478–482.

Liu B, Freyer AM, Hall IP (2007). Bradykinin activates calcium-dependent potassium channels in cultured human airway smooth muscle cells. *Am J Physiol Lung Cell Mol Physiol* **292**: L898–L907.

Liu D, Yang D, He H, Chen X, Cao T, Feng X *et al*. (2009). Increased transient receptor potential canonical type 3 channels in vasculature from hypertensive rats. *Hypertension* **53**: 70–76.

Mason MJ, Mayer B, Hymel LJ (1993). Inhibition of Ca^{2+} transport pathways in thymic lymphocytes by econazole, miconazole, and SKF 96365. *Am J Physiol* **264**: C654–C662.

Meng F, To WK, Gu Y (2008). Role of TRP channels and NCX in mediating hypoxia-induced [Ca(2+)](i) elevation in PC12 cells. *Respir Physiol Neurobiol* **164**: 386–393.

Merritt JE, Armstrong WP, Benham CD, Hallam TJ, Jacob R, Jaxa-Chamiec A *et al*. (1990). SK & F 96365, a novel inhibitor of receptor-mediated calcium entry. *Biochem J* **271**: 515–522.

Moran MM, Xu H, Clapham DE (2004). TRP ion channels in the nervous system. *Curr Opin Neurobiol* **14**: 362–369.

Ohba T, Watanabe H, Murakami M, Takahashi Y, Iino K, Kuromitsu S *et al*. (2007). Upregulation of TRPC1 in the development of cardiac hypertrophy. *J Mol Cell Cardiol* **42**: 498–507.

Okada T, Shimizu S, Wakamori M, Maeda A, Kurosaki T, Takada N *et al*. (1998). Molecular cloning and functional characterization of a novel receptor-activated TRP Ca^{2+} channel from mouse brain. *J Biol Chem* **273**: 10279–10287.

Orestes P, Bojadzic D, Chow RM, Todorovic SM (2009). Mechanisms and functional significance of inhibition of neuronal T-type calcium channels by isoflurane. *Mol Pharmacol* **75**: 542–554.

Panner A, Cribbs LL, Zainelli GM, Origitano TC, Singh S, Wurster RD (2005). Variation of T-type calcium channel protein expression affects cell division of cultured tumor cells. *Cell Calcium* **37**: 105–119.

Romero-Mendez AC, Algara-Suarez P, Sanchez-Armass S, Mandeville PB, Meza U, Espinosa-Tanguma R (2008). Intracellular Ca^{2+}-store depletion triggers a Na^+ influx via SOCs in guinea pig tracheal smooth muscle. *FASEB J* **22** (1_MeetingAbstracts):1206.1.

Rychkov G, Barritt GJ (2007). TRPC1 Ca(2+)-permeable channels in animal cells. *Handb Exp Pharmacol* **179**: 23–52.

Schwarz G, Droogmans G, Nilius B (1994). Multiple effects of SK & F 96365 on ionic currents and intracellular calcium in human endothelial cells. *Cell Calcium* **15**: 45–54.

Self DA, Bian K, Mishra SK, Hermsmeyer K (1994). Stroke-prone SHR vascular muscle Ca^{2+} current amplitudes correlate with lethal increases in blood pressure. *J Vasc Res* **31**: 359–366.

Wang GX, Poo MM (2005). Requirement of TRPC channels in netrin-1-induced chemotropic turning of nerve growth cones. *Nature* **434**: 898–904.

Zhu X, Jiang M, Birnbaumer L (1998). Receptor-activated Ca^{2+} influx via human Trp3 stably expressed in human embryonic kidney (HEK)293 cells. Evidence for a non-capacitative Ca^{2+} entry. *J Biol Chem* **273**: 133–142.